Primljen / Received: 29.5.2020.
Ispravljen / Corrected: 9.10.2020.
Prihvaćen / Accepted: 20.11.2020.
Dostupno online / Available online: 10.2.2021.

Investigation of large-diameter flange joint with soft-gasket

Authors:

Assist.Prof. **Đorđe Jovanović**, PhD. CE
University of Novi Sad, Serbia
Faculty of Technical Sciences
djordje.jovanovic@uns.ac.rs

Assoc.Prof. **Andrija Rašeta**, PhD. CE
University of Novi Sad, Serbia
Faculty of Technical Sciences
araseta@uns.ac.rs
Corresponding author

Assoc.Prof. **Momčilo Spasojević**, PhD. CE
University of Novi Sad, Serbia
Faculty of Technical Sciences
momcilos@uns.ac.rs

Assist.Prof. **Igor Džolev**, PhD. CE
University of Novi Sad, Serbia
Faculty of Technical Sciences
idzolev@uns.ac.rs

Research Paper

Đorđe Jovanović, Andrija Rašeta, Momčilo Spasojević, Igor Džolev

Investigation of large-diameter flange joint with soft-gasket

This study focuses on behaviour of the flanged joint with a soft rubber gasket, which is a common type of gasket for evaporator structures. The assembled structure is tested according to EN 13445-3, and strain values are measured using strain gauges. The numerical analysis in ABAQUS comprises several models with different levels of detail. These models are calibrated according to test data. Recommendations regarding the model complexity that is required to obtain satisfactory prediction of non-linear behaviour of flange joints are presented and documented.

Key words:
flange joint, soft gasket, numerical simulations of joints, large-diameter pressure vessel

Prethodno priopćenje

Đorđe Jovanović, Andrija Rašeta, Momčilo Spasojević, Igor Džolev

Ispitivanje prirubnica velikog promjera s mekom brtvom

U središtu je interesa ovog rada ponašanje spojeva prirubnice i mekane gumene brtve koja je tipična vrsta brtve za isparivače. Montirana konstrukcija ispitala se prema normi EN 13445-3, a naprezanja su se mjerila tenzometrima. Numerička analiza u programskom paketu ABAQUS obuhvaćala je nekoliko modela s različitim detaljima. Ti su modeli bili podešeni u skladu sa zabilježenim podacima iz ispitivanja. U radu su prikazane i dokumentirane preporuke koje se tiču složenosti modela koji je potreban kako bi se postigla zadovoljavajuća razina predviđanja nelinearnog ponašanja spojeva prirubnica.

Ključne riječi:
spoj prirubnice, mekana brtva, numeričke simulacije spojeva, tlačna posuda velikog promjera

Vorherige Mitteilung

Đorđe Jovanović, Andrija Rašeta, Momčilo Spasojević, Igor Džolev

Prüfung von Flanschen mit großem Durchmesser mit Weichdichtung

Der Schwerpunkt dieser Arbeit liegt auf dem Verhalten der Flansch- und Weichgummidichtungsverbindungen, was eine typische Art der Verdampferdichtung ist. Die montierte Struktur wurde gemäß EN 13445-3 geprüft und die Spannungen wurden mit Dehnungsmessstreifen gemessen. Die numerische Analyse im ABAQUS-Softwarepaket umfasste mehrere Modelle mit unterschiedlichen Details. Diese Modelle wurden gemäß den aufgezeichneten Prüfdaten angepasst. Die Arbeit präsentiert und dokumentiert Empfehlungen zur Komplexität des Modells, die erforderlich sind, um eine zufriedenstellende Vorhersage des nichtlinearen Verhaltens von Flanschverbindungen zu erreichen.

Schlüsselwörter:
Flanschverbindung, Weichdichtung, numerische Simulationen von Verbindungen, Druckbehälter mit großem Durchmesser

1. Introduction

Gasket flanges are very common in pressure vessels and piping systems and have been used as such for decades. However, due to versatility in flange types, gasket types and material, and because of special phenomena affecting behaviour of the flange-bolt-gasket systems, exhaustive research work is still required to develop design codes based on real system behaviour. Current codes are almost entirely dependent on experience [1, 2] and, consequently, some problems concerning pipe flange connections have been encountered. The former generation of codes was based on the Taylor-Forge method [3] that was first published in 1937. The design is nowadays governed by the ASME code [4] in the US, and EN 13445-3 [5] in Europe, along with EN 1092-1 [6] for steel flanges and EN 1591-1 [7] for gaskets.

The vast majority of pressure vessels contain a flanged joint, primarily because of prospective disassembly. The design of the joint is driven by sealing performance, maintaining service stress levels below a specified value. An elastic interaction between components is assumed and implicitly included in the analytical approach adopted by the codes. But the complexity of this seemingly simple joint's real behaviour overcomes the one that can be expressed analytically. The gasket is undoubtedly one of main factors that influence behaviour of joints. Design analysis and tightness of flanged joints with metal-to-metal contact has been investigated for a long time [2, 8, 9]. Flanged joints without gasket are mostly used for connecting steel tube sections in civil engineering, where the sealing is much less important than the resistance and load transfer requirements. Recently, Cauchau [10] conducted analytical research using an enriched beam model on a rigid foundation in order to describe the distribution of prying forces, which was later experimentally validated [11]. The stiffness and ultimate resistance of the so called L element [11] is well understood, although not yet completely investigated, as evidenced by recent developments [12, 13]. The introduction of a gasket in the joint, along with the inevitable tightness criterion, necessitates research in several directions. Since pressure vessels are widely used in nuclear power plants, a greater attention was paid to hard gaskets, such as graphite-filled gaskets or metal gaskets [14-16]. Flanges can be made by forging or welding, and while EN 13445-3 recognizes eleven types of flanges, ASME divides them into three groups: loose, integral and optional. On the other hand, the following gasket types can be differentiated: ring, twin, double jacked or full-face gaskets. It is evident that numerous combinations are possible, limiting the effectiveness of universal research of flanged joints and general conclusions.

Many piping flanged joints are standardized and designed as prequalified connections, but the joints should also be divided according to flange radius into small and large-radius joints. The effects of ring behaviour will be much more noticeable in small-radius joints, while large-radius joints are seldom designed as prequalified. Furthermore, elastic interaction of bolt tension during the assembly process also has a significant impact on joint behaviour. An analytical approach for evaluation of interaction is investigated for flange joints of different sizes [17], while a new cost-effective methodology for optimization of tightening sequence has been developed, but only for metallic gasket Ring Type Joints [18]. It should be emphasized that, for small-radius joints, simultaneous preload can be introduced to all bolts, thus avoiding sequential bolt tightening and obtaining a more uniform bolt preload distribution.

Experimental research of a pipe flange connection with the raised face metallic flat gaskets was performed by Sawa et al. [2, 19]. Prying forces in flexible pipe flanged connections were experimentally investigated [8] by determining prying forces based on bolt load measurements. An attempt to measure gasket contact stress distribution using a pressure sensor made of a grid of electrical resistance-conductance ink traces, was made by Bouzid et al. [15]. However, only the qualitative assessment of contact pressure distribution was accomplished. Recently, Luyt [20] measured the gasket contact stresses using the TekScan sensor, for the small-radius flange with only four bolts and the ring type rubber gasket.

Until recently, techniques for measuring gasket contact stresses provided only limited information because of their inherent constraints [15], hence most of the research on the subject was numerical. Fukuoka et al. [21] investigated the tightening process with spring elements, using the 2D flange model. Abid and Nash [22] performed an axisymmetric analysis of flanged joint, by neglecting the bolt holes, and by practically modelling the continuous bolt head ring. Estrada et al. [23] also used the 2D axisymmetric model to investigate contact pressure between the gasket and raised face flange, compensating for bolt holes with softening material in the bolt hole area. Even though these types of models are cost-effective and useful for obtaining some information about joint behaviour, three-dimensional models are far more superior and the only valid type when gasket contact between bolts is of interest. Bouzid and Beghoul [24] adopted a three-dimensional model with solid elements to simulate the raised face flange joint response, using an 18-node solid element for modelling the gasket. Later on, Bouzid and Galai [14] used interface elements for the gasket, namely INTER194 in ANSYS. This was one of a few studies on the behaviour of full-face gasket joints made of soft materials. It provided an analytical approach capable of predicting flange rotation and bolt load change during operation. Several other researchers used 3D models with solid elements. Krishna et al. [25] examined the joint with a spiral wound gasket, using interface elements for the gasket. Similar numerical model adopted by Nelson and Prasad [26] for numerical simulation of joint's behaviour with ring and twin gaskets was also adopted by Do et al. [27] for investigating the influence of gasket modulus in ring-type gaskets. Luyt et al. [20] used solid elements for a gasket with non-linear viscoelastic material model comprised of Neo-Hookean and Prony shear relaxation. In all of the aforementioned three-dimensional numerical models, the pretension in bolts is simulated with pretension elements. Pavlovic et al. [28] modelled bolts (and nuts) as shear studs with threads, and introduced pretension by applying nut rotation in the dynamic explicit solver. Comparing the results from numerical analyses of models with pretension elements and experimental

tests, it can be concluded that the use of pretension elements ensures a sufficiently accurate behaviour. Given that this approach is also more favourable in terms of computational costs, it was further used in the analyses.

The selection of a gasket for the operational conditions and the specification of the assembly procedures should be an integral part of any flange joint design process [1]. This becomes especially important when dealing with a large-diameter joint structure with soft gasket. To the best of authors' knowledge, test results of this particular situation have not as yet been reported in the literature. This is the main motivation for this study, along with another peculiarity of the examined structure; namely, the fact that flange stiffeners are usually used in typical (prequalified) small-diameter pipe connections, but their influence on large-diameter flanges soft gasket has not been directly investigated.

This paper deals with the structure that encompasses all above mentioned peculiarities. The structure was built and it is operating but, during the testing phase, measuring equipment was installed and strains in the proximity of the flange were measured, in order to calibrate a precise three-dimensional numerical model of the structure. This model is used as a basis for further study of the influence of stiffeners and soft gasket parameters on joint behaviour.

2. Details of structure and measurements

2.1. Description of structure

The tested vessel structure is used as a part of the technological equipment for a sugar refinery (Figure 1). During operation, in addition to self weight, the structure is filled with sugar syrup at the temperature of 140 °C that is 5 m high from the bottom head. The vessel testing procedure includes filling the vessel with water up to 5 m and exposing it to an overpressure of 400 kPa. The steel structure of the vessel consists of a cylindrical shell 4600 mm in outer diameter and 9000 mm in length. Up to a height of 5000 mm, the shell thickness is 14 mm, and above this height the shell is 12 mm in thickness. Two torispherical heads on both ends of the cylinder are 945 mm high and 12 mm thick. The structure is supported on 4 equally spaced radially arranged lugs. The cylindrical shell is stiffened at the contact zone with the support lugs using 20 mm-thick steel plates. The lugs consist of steel plates 20-30 mm in thickness.

An axially mounted tube with the outer diameter of 1428 mm is placed inside the cylindrical shell. Two ring steel plates 30 mm in thickness are placed at both ends of the tube. The plates are perforated with circular holes (35 mm in diameter) in which a total of 7750 steel pipes are placed, with an outer diameter of 35 mm and wall thickness of 1.5 mm.

The bottom plate is extended radially by 100 mm, forming a steel flange perforated with holes for bolt connection with the bottom head (Figure 1). Another steel flange 30 mm in thickness is welded to the bottom head.

Between the bottom plate and cylindrical shell, thirty-five steel stiffeners equally distributed along the circumference of the vessel are welded from the outside of the upper and lower flange. Four bolts are placed between every two consecutive stiffeners. The radial position of stiffeners on both flanges coincides. The stiffeners are 12 mm in thickness. The connection between the flanges is established with 140 bolts. The upper flange is a blind flange, welded to the shell with two 12 mm-thick fillet welds. The same welds are used to connect the bottom head to the bottom flange. A silicon rubber gasket 100 mm in width and 5 mm in thickness is placed between the two flanges. The upper head is welded to the cylindrical shell.

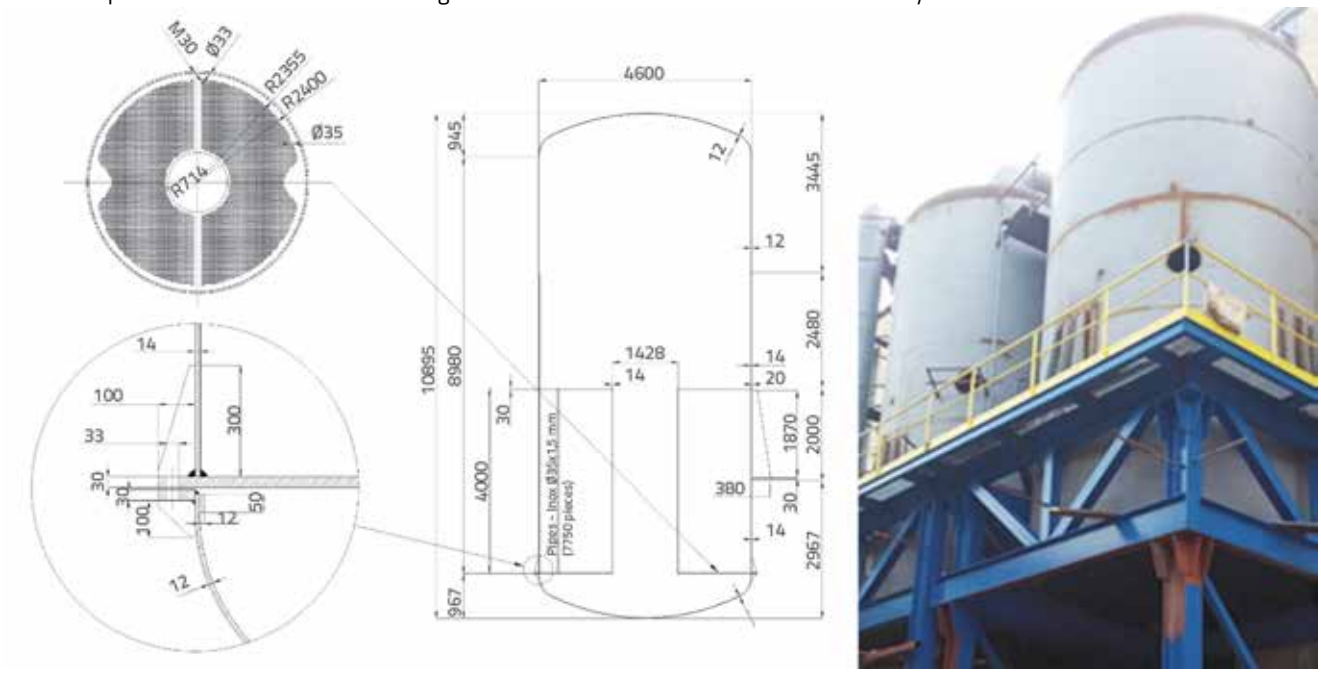

Figure 1. The tested structure of the vessel (right) and a detail of the lower steel plate (left)

Steel material P355 GH is used for constructing the shell, heads, plates, flanges, inner tube, lugs, stiffeners and inner pipes; material properties are E = 200 GPa, ν = 0.3, f_y = 355 MPa and f_u = 510 MPa. The bolts are M30, class 8.8. Mechanical properties of the silicone rubber gasket are experimentally determined as described in the following section.

2.2. Testing procedure

2.2.1. Gasket material testing

In pressure vessels with a soft gasket, mechanical properties of the gasket strongly influence flange behaviour, as well as the tightness of connection. Several tests are prescribed for testing rubber material, such as the tensile test, simple compression test, volumetric compression (bulge test), plane strain compression test, plane strain tension test, equibiaxial tension test, durometer hardness test, etc. Although the use of the equibiaxial tension test is advised for a more accurate determination of material response to uniaxial compression, the simple compression test is used herein, under the actual operating conditions of the vessel.

A gasket sample measuring 50x50x5 mm (taken from the same batch as the one incorporated in the structure), was tested. Using steel plates connected to the hydraulic press, the pressure force was applied at a rate of 2 kN/min until the maximum force of 50 kN was reached, with an accuracy of 10 N. The lower steel plate was fixed and displacement of the upper plate was measured with LVDT with an accuracy of 10^{-6} m (Figure 2). The test was conducted both with and without application of lubricant to the contact surfaces. In case of unlubricated contact, during unloading, the specimen retained deformed shape until complete unloading, after which it abruptly returned to its original shape. The force-displacement curve could not be adequately determined and, therefore, the tests were further conducted with lubricated contact only, providing force-displacement curve for both loading and unloading stages. Results are obtained in the force-displacement form, to be later used for the calculation of material parameters in ABAQUS (Section 3.1).

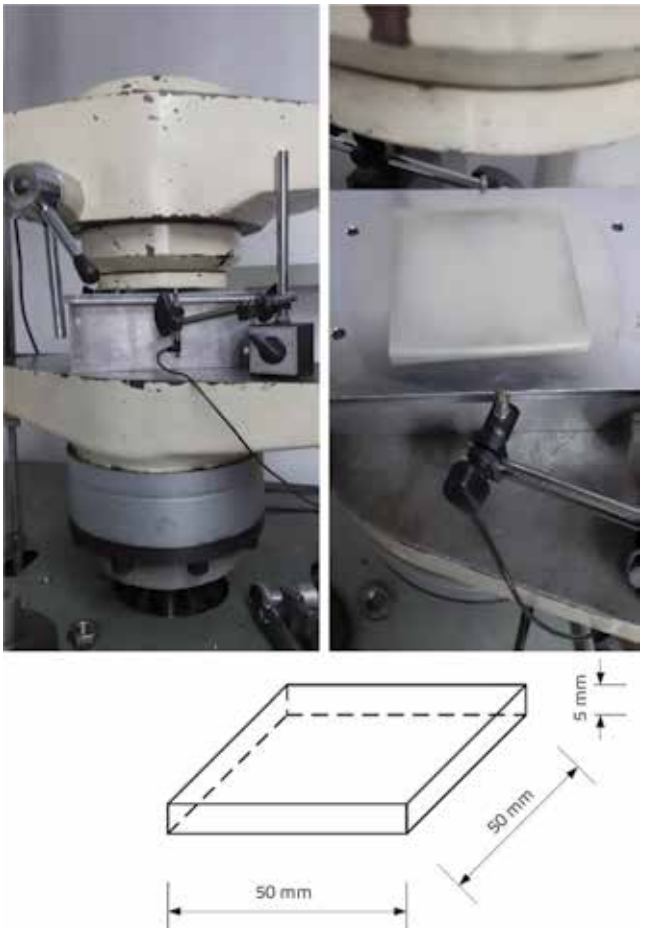

Figure 2. Uniaxial compression test of gasket material

2.2.2. Pressure vessel testing

The experimental testing procedure of the vessel was conducted in situ. Measuring devices were placed according to the scheme provided in Figure 3. Linear strain gauges (marked as S1) were used at some positions. Rosette gauges (marked as S2, S3 and S4) were used at other locations in order to measure strains in two orthogonal directions. The data acquisition system Quantum X (by Hottinger-Baldwin Messtechnik (HBM)

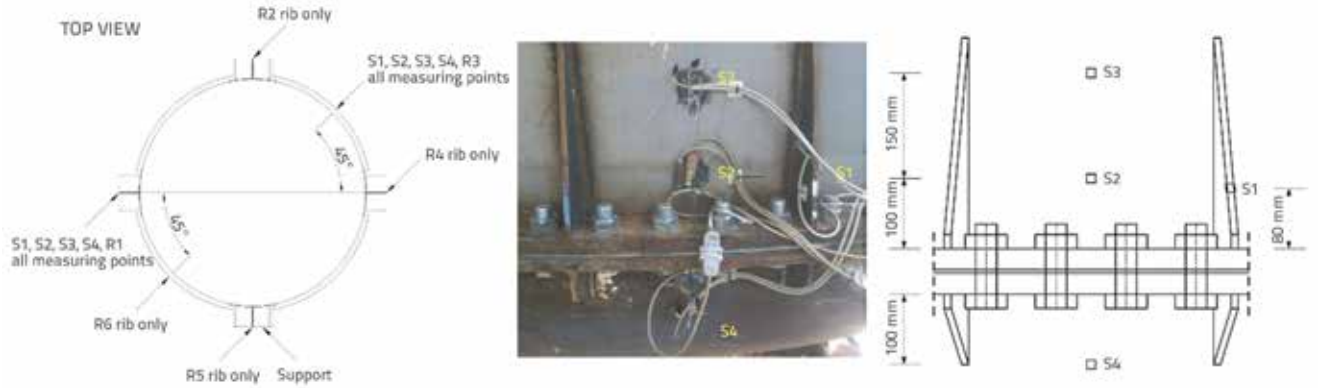

Figure 3. Location of strain gauges – circumferential positions (left) and vertical positions (right)

Company) was used. The strain gauges were also manufactured by the HMB company.

The loading sequence consisted of several stages. After assemblage of the bottom head, bolts were tightened to a pre-tension force of 160 kN per bolt, in two passes, according to the design. The vessel was then filled with water up to the upper steel plate and exposed to an overpressure of 400 kPa. The loading sequence is shown in Table 1. The measurement data were collected for all loading stages. However, the data from the first two stages showed a rather low level of strain that is susceptible to noise interference. As a result, only the data from the third stage were used for calibration of the numerical model.

Table 1. Loading sequence of pressure vessel

Phase	Loading
I	Bolt pretension + self-weight
II	I + water pressure up to the upper steel plate level
III	II + testing overpressure

3. Finite element modelling

The structure was analysed using the software ABAQUS [29], based on the finite element method. Due to two-plane symmetry, only 1/4 of the structure was modelled (Model A), with the corresponding boundary conditions. Furthermore, an additional model concerning axial symmetry was developed in order to produce a more computationally efficient solution for the subsequent nonlinear analysis. This model was aimed at reducing the overall number of degrees of freedom, while keeping the mesh quality and element size unchanged (Figure 4), by modelling only 1/35 of the structure in the tangential direction, including a zone between two subsequent stiffeners with four bolts in between (Model B).

Although the axisymmetric model would assume distributed support along the circumference of the cylindrical shell, which is arguable in the real boundary conditions, the results of the two models are compared in order to confirm that the modifications of the support distribution do not affect the zone of interest, i.e., the connection between the cylindrical shell and bottom head. Table 2 presents the range of Von-Mises stress in tangential directions, in the zone of Region 1 and 2 (Figure 5), as well as the vertical displacement u_z of the bottom head centre, for models A and B, at the third stage of loading (Table 1). For each model, the differences between extreme stresses in the tangential direction are not larger than approximately 5 %. Based on that, the axisymmetry (Z-axis) is achieved. Also, differences in stress between models A and B are not greater than approximately 2 %, and displacements are practically the same, leading to a conclusion that the use of model B in further analysis of the connection would be justified.

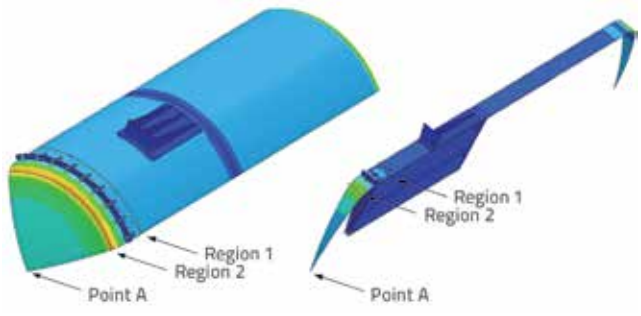

Figure 5. Distribution of Von-Mises stress results in regions 1 and 2 and displacement of point A

Results presented in Table 2 are obtained using the elastic analysis, assuming bonded contact between all parts of the vessel, with material properties of steel corresponding to P355 GH, and gasket properties E = 0.003 GPa and ν = 0.49. All inner pipes are discretized using elements S4R and all other elements of the vessel using C3D8R elements. The finite element model is presented in Figure 6.

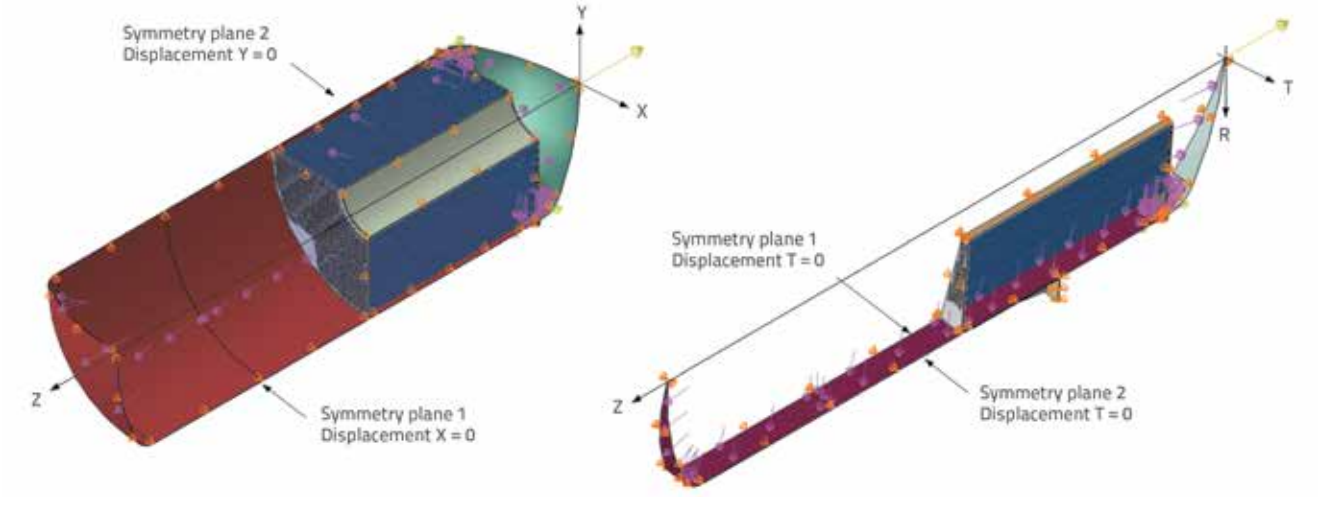

Figure 4. Model A (left) and Model B (right)

Table 2. Comparison of elastic analysis results for two models, concerning two-plane and axi-symmetry

Model \ Results	σ [MPa]		u_z [mm]	**Analysis duration** [min]
	Region 1	Region 2	Point A	
Model A	61 – 63	246 – 251	6.22	25704
Model B	60 – 63	245 – 250	6.21	1071

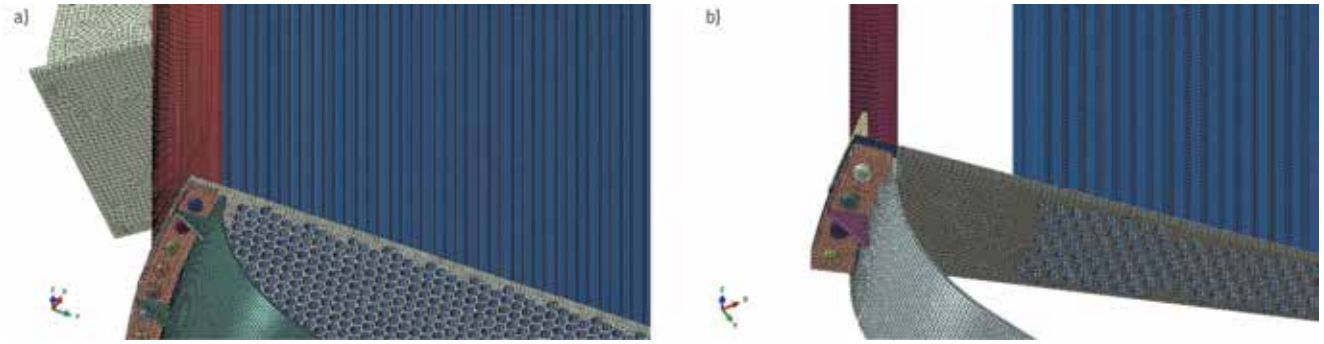

Figure 6. Finite element model – Model A (left) and Model B (right)

The axisymmetrical model (model B) was adopted as a basis for development of a more advanced model for nonlinear analysis, including contact formulation between bolts and flanges, gasket and flanges, as well as nonlinear material properties of the gasket, and taking into account geometric nonlinearity.

3.1. Gasket modelling for nonlinear analysis

Only 1/8 of the setup is modelled, including three plane symmetry (Figure 7). The steel plate (elastic behaviour) is meshed using C3D8R elements, while the gasket behaviour is modelled using a nonlinear hyper-elastic material model, with C3D8HR elements. Experimental data is fitted using the Mooney-Rivlin [30] material model. The gasket mechanical properties in FEM model are calibrated based on results of test procedure described in Section 2.2.1.

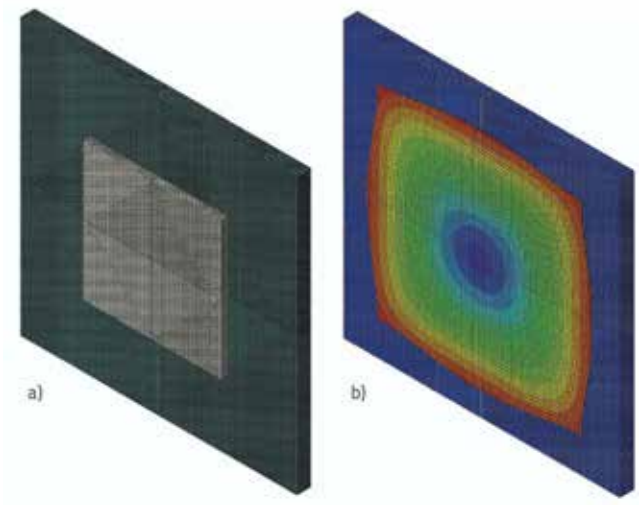

Figure 7. FEM model for validation of gasket material model: a) početno stanje; b) zbijeno stanje

The gasket is modelled including the Mullins effect [29, 31]. Stress softening, which is commonly observed in elastomers (as a result of damage associated with straining), is introduced by using two numerical parameters; namely, r and m [32]. They represent a measure of the extent of the damage relative to virgin state, and the dependence of the damage on the extent of deformation, respectively. The extension of the Ogden and Roxburgh [32] damage variable also includes the parameter β, which could be used for overcoming convergence difficulties for overly stiff response at the initiation of the unloading stage, as was observed during the experiment. Gasket material parameters are presented in Section 4.1. The contact between the steel plate and gasket is modelled as a hard frictional contact [29], which minimizes the penetration of slave surface into master surface at the constraint locations and does not allow transfer of tensile stress across the interface. The adopted low coefficient of friction μ = 0.03 corresponds to the conditions in the experiment.

3.2. Vessel modelling for nonlinear analysis

For nonlinear analysis, all contact surfaces are defined as frictional, with higher friction coefficients of 0.3 and 0.5, between bolts and flanges, and between the gasket and flanges, respectively (Figure 8).

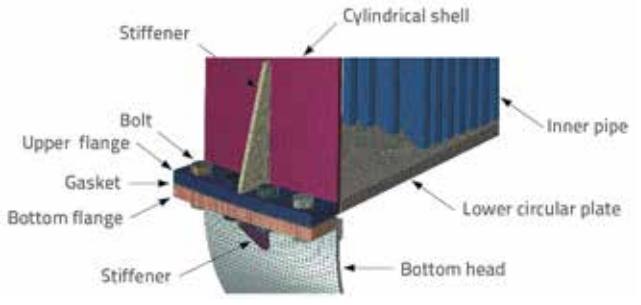

Figure 8. FEM model for nonlinear analysis

All other vessel parts are fully bonded. Inner pipes are discretized using S4R elements, the gasket with C3D8HR and all other elements with C3D8R. Across the thickness of the elements, stiffeners are discretized with one layer of elements, whereas the bottom and the upper head, as well as the cylindrical shell, are discretized with two layers of elements. Three elements are used across the upper and lower circular plates, while the bottom flange and gasket use five layers of elements. Load steps are defined according to the testing procedure (Table 2).

4. Results and discussion

4.1. Calibration of numerical model

The comparison between the results obtained by the gasket FEM model and experimental data are presented in Figure 9.

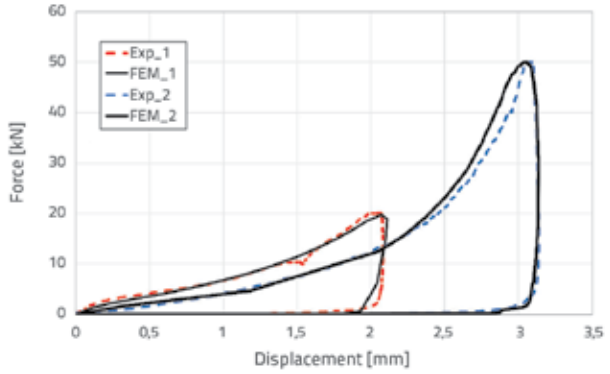

Figure 9. Gasket force-displacement relation

Based on measured data, the FEM model is calibrated in order to determine the input parameters that would provide good agreement with the measured data. Parameters adopted for the Mooney-Rivlin material model are: C_{10} = 453 kPa, C_{01} = 113 kPa and D_1 = 0. Numerical analysis is conducted including the Mullins effect, with parameters: r = 0.1, m = 0.1 and β = 0.1. The contact between steel plates and rubber is defined as frictional, with a coefficient of friction μ = 0.03.

The same gasket material model is implemented in nonlinear analysis of the vessel structure. The loading sequence used in numerical analysis follows the testing procedure (Table 1). Results obtained by experimental measurements and the finite element analysis are presented in Table 3.

4.2. Flange and gasket behaviour

A parametric study was performed using the calibrated model of the vessel in order to investigate the influence of soft-gasket material properties, as well as the influence of the number of stiffeners. Stiffeners are used primarily to strengthen large-diameter flanges and avoid large flange rotations that affects bolts pre-tensioning due to the deformability of the flange on top of the elastic interaction. In connections with small-diameter flanges, stiffeners are designed between each pair of adjacent bolts. Since there are 140 bolts in the examined flange, the same number of stiffeners and accompanying welds would be excessive. On the other hand, if the stiffeners are overly spaced out, their strengthening influence would be diminished. Stiffener spacing may be equal to four times the bolt spacing in many designs. Yet, in the parametric study, three spacing scenarios are investigated (Table 4), namely (1) four bolts are placed between two adjacent stiffeners (G1-S4), (2) stiffener spacing is equal to bolt spacing, so there is a bolt between each two adjacent stiffeners (G1-S1), and (3) stiffeners are omitted, in order to evaluate their overall influence on the flange operational behaviour (G1-S0).

Table 4. Parametric analysis models analysing the influence of stiffeners and gasket type

No.	Model description	Mark
1	Calibrated gasket type 1 (C_{10} = 453 kPa, C_{01} = 113 kPa) Four bolts placed between two consecutive stiffeners	G1-S4
2	Calibrated gasket type 1 (C_{10} = 453 kPa, C_{01} = 113 kPa) One bolt placed between two consecutive stiffeners	G1-S1
3	Calibrated gasket type 1 (C_{10} = 453 kPa, C_{01} = 113 kPa) Without stiffeners	G1-S0
4	Gasket type 2 (C_{10} = 372 kPa, C_{01} = 93 kPa) Four bolts placed between two consecutive stiffeners	G2-S4
5	Gasket type 3 (C_{10} = 534 kPa, C_{01} = 133 kPa) Four bolts placed between two consecutive stiffeners	G3-S4

Table 3. Results of experimental and numerical analysis of the vessel (difference between loading stages II and III)

Average values	Model			
	MEASURED Four bolts placed between two consecutive stiffeners	**FEA Four bolts placed between two consecutive stiffeners**	**FEA without stiffeners**	**FEA One bolt placed between two consecutive stiffener**
Measuring place	μm/m	μm/m	μm/m	μm/m
Free edge along the rib				
S1	469	464	/	195
Horizontal direction				
S2	-172	-143	248	-95
S3	-122	-109	100	-78
S4	38	35	135	22

Table 5. Influence of stiffeners on Von-Mises stress values in the vessel and contact pressures in the gasket

Model	W/o stiffeners (G1-S0)	1 bolt between 2 adjacent stiffeners (G1-S1)	4 bolts between 2 adjacent stiffeners (G1-S4)
Stress at S2 strain gauge [MPa]	36 Osnovna linija	60 +67 % ↑	58 +61 % ↑
Contact pressure in gasket next to bolt [MPa]	16.3 Osnovna linija	15.8 -3.1 % ↓	15.9 -2.3 % ↓
Contact pressure in gasket between bolts [MPa]	13.4 Osnovna linija	14.4 +7.5 % ↑	14.2 +6 % ↑

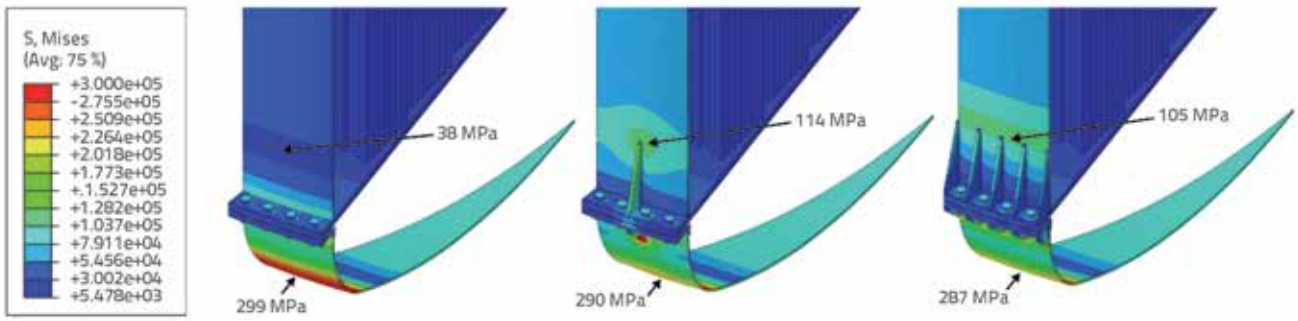

Figure 10. Von-Mises stress distribution depending on position of stiffeners

Results, in terms of Von-Mises stress at the end of stage III (Table 1) for the position of S2 strain gauge (Figure 3) are presented in Table 5 and Figure 10. The same is the case with contact pressure in the gasket in tangential direction, next to the bolts and in between the bolts, for the same gasket properties (denoted by C_{10} = 453 kPa and C_{01} = 113 kPa), as presented in Table 5 and Figure 10.

On the other hand, for a soft gasket, as used in the considered structure, the material stress-strain law plays a crucial role in the flange response. Additionally, only the Shore hardness is provided by the manufacturer for the silicone rubber material used as a gasket. This parameter, neglecting its nominal character, is neither sufficient to provide necessary data about rubber behaviour, nor can it be considered accurate. In [33], the relationship between the Shore hardness (s) and elastic modulus (E) is proposed in the form:

$$E = \frac{0.0981 \cdot (56 + 7.66s)}{0.137505 \cdot (254 - 2.54s)} \quad \text{[MPa]} \qquad (1)$$

This expression has been proven fairly accurate by Methhananda et al. [33] and, with simple relation for conversion of Young's modulus to the Neo-Hookean parameter, it would be possible to define a simple rubber material model in FEM analysis. However, the Neo-Hookean model with Mullins effect is not used in this study, since the Mooney Rivlin model provides better fit with experimental data, primarily in the unloading part of the force-displacement path.

Independently of the number of parameters used to describe soft gasket material, some distribution is expected. This distribution is most often predicted as normal distribution, and is applied in developing safety coefficients for materials, which are used in technical provisions and codes. Also, as proven for large diameter spiral wound gaskets in [34], the behaviour of the full gasket and behaviour of a single sector of the gasket showed a high discrepancy. Additionally, this study showed that measurements are not carried out with the most accurate procedure by the manufacturers. This could also be the case of rubber gaskets. In order to investigate the influence of gasket material properties on flange behaviour, these properties were varied, and the calibrated numerical model was analysed under such conditions. Therefore, a very modest sensitivity analysis of the tested structure was performed by using the one-at-a-time (OAT) method, and by investigating the effects of two variables: the number of stiffeners, and gasket stiffness. The method for varying the number of stiffeners has already been explained but, in order to define meaningful increment for gasket material modification, it would be desirable to possess some knowledge of the rubber-strength variation coefficient. For example, according to Eurocodes, the coefficient of variation (CoV) for steel yield strength amounts to 0.07 [35]. However, to the extent of the authors' knowledge, there are no similar recommendations for rubber material. Consequently, a relatively high CoV is assumed – 0.09, and differences between the mean value and 5 % and 95 % fractiles were used, leading to 17.3 % of stiffness variation, both positive and negative. The results of these analyses are presented in Figure 11, where flange rotation in the radial direction is depicted. Although variation of Mooney-Rivlin parameters affects the gasket stiffness, the influence on the stiffness ratio between gasket and steel flange with bolts is not significant, resulting in a very similar response of the flange rotation in all three analysed cases (G1-S4, G2-S4 and G3-S4). The length of flange is measured from the outer flange edge.

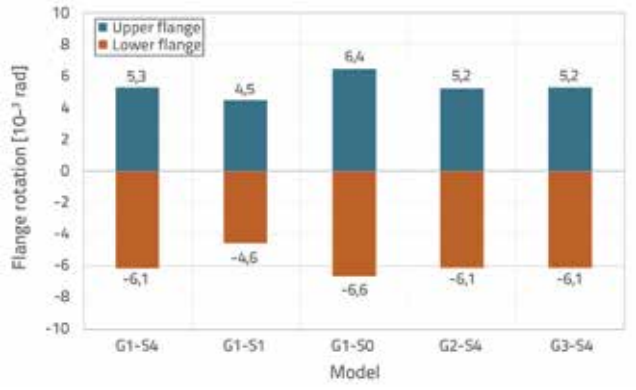

Figure 11. Rotation of flanges at the end of stage III for different stiffener positions and gasket material properties

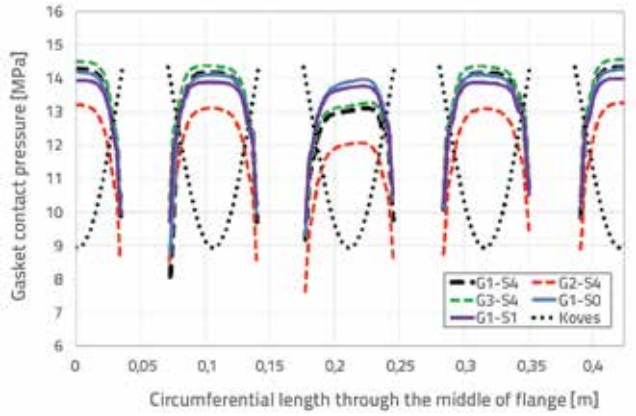

Figure 12. Gasket contact pressure variation in circumferential direction through centre of bolts

Gasket contact pressures in circumferential directions of the analysed models are presented in Figure 12. The contact pressure in the gasket has the smallest value right next to the bolt hole, and the highest value in the middle between two holes. This is the consequence of incompressibility of the gasket material, and its high deformability. The rubber gasket is extruded out in these regions due to high pressures perpendicular to the mid-surface. As it can be observed from the results, softer gasket (gasket type 2) exhibits smaller sealing pressures throughout the length, as the contact pressure profile in Figure 12 is translated down the ordinate axis. The same translation, but in a much smaller amount, is observed in the case of a harder gasket material (gasket type 3). Compared to this, the influence of the number of stiffeners on the contact pressure is lower, as all variations regarding the quantity of the stiffeners produce contact pressures between the ones for medium and harder gaskets. It can be concluded that gasket material has the strongest influence on sealing pressure, and that it becomes more pronounced as the gasket gets softer. The gasket contact pressure predictions calculated by the method presented by Koves [37] are also depicted in Figure 12. It is evident that the distribution of these stresses is almost as converse to the numerical results. This is because the Koves' method is derived from the assumption of the beam (flange) on an elastic foundation (gasket). The same assumption is used in similar work by Dan, Bouzid and Dao [36]. However, due to the extreme differences in stiffness between the flange and rubber gasket, and the incompressibility of the gasket, contact stresses are almost completely determined by the gasket behaviour. These types of discrepancies were not accounted for in the Koves' formula, which has primarily been developed for hard gaskets. In the presented results of the Koves' method, the adopted elastic modulus of the gasket is 1.5 MPa, which corresponds to the secant modulus of the gasket for the expected stress values. This is calculated from the force-displacement curve presented in Figure 9. The comparison of the numerical and analytical results strongly suggests that Koves' formula does not apply to soft gasket material.

5. Conclusion

Flange joints in pressure vessels have been studied for a very long time, as they represent an almost indispensable part of every pressure vessel structure. Since pressure vessels are used in many fields, greater attention is dedicated to the analysis of flanges with stronger and more enduring gaskets. But in the food industry, rubber gaskets are very common. Strain measurements of sugar evaporator during its initial test are presented in this paper. A large-diameter flange was designed with stiffeners, in order to obtain greater stiffness. Then, several numerical models of the whole structure were made and the results were compared with the measured data. It was established that it is more effective to disregard modest asymmetry and model only the section of the vessel. Results are very similar, but the major advantage in this case is the possibility to model the gasket behaviour with a much more sophisticated model and to include contacts which, in the case the entire structure is modelled, would involve an exceptional computational and time effort.

The flange stiffeners are disregarded for large-diameter flanges in almost all design codes. The stiffness of the upper flange and the cylinder, as well as the lower flange and the bottom head, is such that bolt pretensioning does not induce significant bending of the flanges in circumferential direction. Although stiffeners increase an overall stiffness, they do not affect the gasket contact pressures significantly. However, the stiffeners transmit considerable stresses, and hence induce additional bending in the adjoining cylinder wall. The number of stiffeners along radial direction is varied and the results of their influence on both gasket pressure and cylinder wall stresses are presented. Based on the analyses results, it can be concluded that the presence of stiffeners does not affect flange behaviour significantly, but that it affects stresses in the cylinder.

The silicone rubber gasket significantly affects the flange behaviour and flange tightness. In this study, the gasket material is separately tested under conditions similar to operational ones – a simple compression test was performed by applying lubricant to the rubber surfaces. The friction between metal flanges and rubber gasket mainly affects the unloading behaviour of the gasket. It is also concluded that accurate predictions of the gasket behaviour (and consequently flange joint behaviour) are difficult to obtain if the Neo-Hookean model for rubber is used. The Mooney-Rivlin model

with Mullins effects has provided satisfactory results. Considering the above said, it is concluded that in the case of a soft gasket, or stiffened large-diameter flanges, due to many nonlinearities involved, it is hard to predict contact stresses and flange rotation via simple expressions provided in codes or even analytical formulas such as the one proposed by Koves. Hence, sophisticated numerical analyses, such as the one that is thoroughly presented in this paper, are considered advantageous.

Acknowledgements

This research has been conducted within the scientific research project *Multidisciplinary theoretical and experimental research in education and science in the fields of civil engineering, risk management and fire safety and geodesy*, developed at the Department of Civil Engineering and Geodesy, Faculty of Technical Sciences, University of Novi Sad, Serbia.

REFERENCES

[1] Brown, W., Derenne, M., Bouzid, A.H.: The Effects of Thermal Loading on Pressure Vessel Flanged Joints, European Symposium on Pressure Equipment - ESOPE 2001, Paris, France, 2001, pp. 416-425.

[2] Sawa, T., Higurashi, N., Akagava, H.: A Stress Analysis of Pipe Flange Connections, Journal of Pressure Vessel Technology 113 (1991), pp. 497-503.

[3] Modern Flange Design, Bulletin 502, G&W Taylor-Bonney Division, 1978.

[4] A.B.a.P.V. Committee, ASME VIII, Rules for Construction of Pressure Vessels, Division 1, New York, USA, 2013.

[5] CEN, EN 13445-3: Unfired pressure vessels - Part 3: Design, European committee for standardization, Brussels, Belgium, 2014.

[6] CEN, EN 1092-1: Flanges and their joints - Circular flanges for pipes, valves, fittings and accessories, PN designated - Part 1: Steel flanges, European committee for standardization, Brussels, Belgium, 2018.

[7] CEN, EN 1591-1:2013: Flanges and their joints - Design rules for gasketed circular flange connections - Part 1: Calculation, European committee for standardization, Brussels, Belgium, 2013.

[8] Huang, F., Zhang, D., Hong, W., Li, B.: Mechanism and calculation theory of prying force for flexible flange connection, Journal of Constructional Steel Research, 132 (2017), pp. 97-107.

[9] Meck, H.R.: Analysis of Bolt Spacing for Flange Sealing, Transactions of ASME, (1969), pp. 290-292.

[10] Couchaux, M., Hjiaj, M., Ryan, I.: Static resistance of bolted circular flange joints under tensile force, (2010), pp. 27-35.

[11] Couchaux, M., Hjiaj, M., Ryan, I., Bureau, A.: Tensile resistances of L-stubs, Journal of Constructional Steel Research, 138 (2017), pp. 131-149.

[12] Pavlović, M., Heistermann, C., Veljković, M., Pak, D., Feldmann, M., Rebelo, C., Simões da Silva, L.: Connections in towers for wind converters, part I: Evaluation of down-scaled experiments, Journal of Constructional Steel Research, 115 (2015), pp. 445-457.

[13] Couchaux, M., Hjiaj, M., Ryan, I., Bureau A.: Effect of contact on the elastic behaviour of tensile bolted connections, Journal of Constructional Steel Research, 133 (2017), pp. 459-474.

[14] Bouzid, A.H., Galai, H.: Bolted Flange Joints with Full Face Gaskets: An analytical approach based on flexibility, Proceedings of 2005 ASME Pressure Vessels and Piping Division Conference, Denver, Colorado, USA, 2005, pp. 29-35.

[15] Bouzid, A.H., Derenne, M.: Analytical Modeling of the Contact Stress With Nonlinear Gaskets, Journal of Pressure Vessel Technology, 124 (2002) 1, pp. 47.

[16] Svhneider, R.W.: Flat Face Flanges With Metal-to-Metal Contact Beyond the Bolt Circle, Transactions of ASME, (1968), pp. 82-88.

[17] Zhu, L., Bouzid A.H., Hong J.: Analytical evaluation of elastic interaction in bolted flange joints, International Journal of Pressure Vessels and Piping, 165 (2018), pp. 176-184.

[18] Coria, I., Abasolo, M., Olaskoaga, I., Etxezarreta, A., Aguirrebeitia, J.: A new methodology for the optimization of bolt tightening sequences for ring type joints, Ocean Engineering, 129 (2017), pp. 441-450.

[19] Sawa, T., Hiroyuki, K.: On the Characteristics of Bolted Joints with Gasket, Bulletin of JCME, 28 (1985) 237, pp. 400-407.

[20] Luyt, P.C.B., Theron, N.J., Pietra, F.: Non-linear finite element modelling and analysis of the effect of gasket creep-relaxation on circular bolted flange connections, International Journal of Pressure Vessels and Piping, 150 (2017), pp. 52-61.

[21] Fukuoka, T.: Analysis of the Tightening Process of Bolted Joint With a Tensioner Using Spring Elements, Journal of Pressure Vessel Technology, 116 (1994), pp. 443-448.

[22] Abid, M., Nash D.H.: Comparative study of the behaviour of conventional gasketed and compact non-gasketed flanged pipe joints under bolt up and operating conditions, International Journal of Pressure Vessels and Piping, 80 (2003) 12, pp. 831-841.

[23] Estrada, H.: Analysis of Leakage in Bolted-Flanged Joints Using Contact Finite Element Analysis, Journal of Mechanics Engineering and Automation, 5 (2015) 3, pp. 135-142.

[24] Bouzid, A.H., Beghoul, H.: The design of Flanges based on Flexibility and Tightness, Proceedings of PVP2003 ASME Pressure Vessels and Piping Conference, Cleveland Ohio, USA, 2003, pp. 31-38.

[25] Murali Krishna, M., Shunmugam, M.S., Prasad, N.S.: A study on the sealing performance of bolted flange joints with gaskets using finite element analysis, International Journal of Pressure Vessels and Piping, 84 (2007) 6, pp. 349-357.

[26] Nelson, N.R., Prasad, N.S.: Sealing behavior of twin gasketed flange joints, International Journal of Pressure Vessels and Piping, 138 (2016), pp. 45-50.

[27] Do, T.D., Bouzid, A.H., Dao, T.M.: Effect of Bolt Spacing on the Circumferential Distribution of the Gasket Contact Stress in Bolted Flange Joints, Journal of Pressure Vessel Technology, 133 (2011) 4, 041205.

[27] Pavlović, M., Marković, Z., Veljković, M., Buđevac, D.: Bolted shear connectors vs. headed studs behaviour in push-out tests, Journal of Constructional Steel Research, 88 (2013), pp. 134-149.

[28] A.U.M.V. 6.9., DS SIMULIA Corp, Providence, RI, USA, 2009.

[29] Mooney, M.: A Theory of Large Elastic Deformation, J. Appl. Phys, 11 (1940), pp. 582–592.

[30] Mullins, L.: Softening of rubber by deformation, Rubber Chem Technol, 42 (1969), pp. 339–362.

[31] Ogden, R.W., Roxburgh, D.G.: A pseudo-elastic model for the Mullins effect in filled rubber, Proc. R. Soc. Lond, A 455 (1999), pp. 2861-2877.

[32] Meththananda, I.M., Parker, S., Patel, M.P., Braden, M.: The relationship between Shore hardness of elastomeric dental materials and Young's modulus, Dental materials: official publication of the Academy of Dental Materials, 25 (2009) 8, pp. 956-959.

[33] Delaunay, Y., Fontaine, Y.: Large diameter spiral wound gasket behavior, measured on the entire gasket and on small gasket sectors, ASME 2005 Pressure Vessels and Piping Conference, Denver, Colorado USA, 2005, pp. 67-73.

[34] Implementation of EUROCODES - Handbook 2, Prague, Czech Republic, 2005.

[35] Dan Do, T., Bouzid, A.H., Dao, T.M.: Development of a New Bolt Spacing Formula, Journal of Pressure Vessel Technology, 136 (2013) 1, 011206.

[36] Koves, W.J.: Flange Joint Bolt Spacing Requirements, Proceedings of 2007 ASME Pressure Vessels and Piping Division Conference, San Antonio, Texas, 2007, pp. 3-10.